Spatially Resolved Characteristics of Pharmaceutical Sprays

A. R. Muliadi* and P. E. Sojka
Maurice J. Zucrow Laboratories—School of Mechanical Engineering
Purdue University
West Lafayette, IN 47906

Abstract

The inter-tablet variation in pharmaceutical tablet film-coating quality is attributed to spatial variations in spray mass and droplet wetting characteristics. The latter is governed by the size and velocity of the drops when they impact the tablets. Accordingly, spray data that show how spatial distributions of spray mass, drop size, and drop velocity vary with changes in spraying conditions are important, and are the subject of this study. In particular, this study characterized sprays produced by two different pharmaceutical nozzles (Schlick 930 and 970). Data show that all drop size distributions have small drops near the spray center and large ones at the periphery, and that drop velocity profiles are Gaussian, often with an offset peak. As expected, drop size decreases as atomizing air supply pressure increases, or when coating supply rate or viscosity decreases. Drop velocity decreases with increasing coating supply rate or an increase in gun-to-target distance, and increases with an increase in air supply pressure. Interestingly, an increase in shaping air pressure increases drop velocity for the 970 sprays, but decreases it for the 930 ones. There were four spray volume flux distributions: dumbbell-shaped, teardrop-shaped, elliptical with a maximum at the spray center, and elliptical with no distinct maxima. The length of the semi-major axis, as well as the distance separating the two maxima, increase with increasing coating supply rate or viscosity; both decrease as atomizing air pressure increases. Spray volume flux increases as coating supply rate or air supply pressure increases, and decreases as coating viscosity or gun-to-target distance increases.

Introduction

Most pharmaceutical tablets have a thin film coating on their surface. It's often of significant importance as it may mask taste, improve mechanical properties, separate reacting ingredients within the tablet, ease swallowing, seal the tablet from moisture to improve shelf-life, and/or control drug release rate and location within the patient.

Film coat is usually applied by subjecting the tablets to an atomizer-produced spray while tumbling them inside a rotating circular drum. Current implementation of this process, however, is such that film finish defects (e.g. cracks/splits in films, film peeling off tablet surfaces, poor film-to-tablet adhesion, etc.) and inter-/intra-tablet coating non-uniformities often occur. Measurements show that film thickness varies, on average, by as much as 57% from one tablet to another [1]. This is a significant problem, especially when the film coat controls the release-rate and/or release-location of the active ingredients. In such cases, the drug may be released too early—when a portion of the film coat is too thin, or when it is missing altogether—or too late, when the film coat is too thick.

Available literature confirms that tablet film quality is strongly influenced by the operating parameters gun-to-bed distance, coating supply rate, atomizing air supply pressure, spray shape (pattern), and coating viscosity. Previous investigations that considered these issues include: [2-4], who found that increasing atomizing air pressure or decreasing gun-to-target distance resulted in a smoother film coat; [2] and [3], who found that film-to-tablet adhesion decreased as coating viscosity increased; [4] and [5], who found that increasing the local spray mass flux at the tablet bed, which can be achieved by increasing the coating supply rate or by changing the spray pattern from an elliptical to a circular shape, decreased the incidence of film splitting; [6], who confirmed that increasing atomizing air pressure decreased intra-tablet film thickness variations; and [7] and [8], who noted more inter-tablet film thickness variation when atomizing air pressure [7, 8], coating viscosity, or coating supply rate rose [8].

The phenomena described above can be explained by droplet wetting characteristics [4, 9] and by understanding how mechanical stresses are developed in film coatings [9-11]. Those described in [7,8], however, likely arise from non-uniformities in sprays [1]. Most currently available spray data provide only qualitative assessment of spray uniformity. Some examples are [7] and [8], in which it was speculated that spray non-uniformities are exacerbated when the atomizing air pressure is increased. No quantitative measurements, however, were taken in either [7] or [8]. Studies that do provide quantitative measurements of spray size/velocity/flux distributions are limited to measurements along the spray's semi-minor or semi-major axis [4, 12]. Moreover, few quantitative data are available as to how spray non-uniformities vary with commonly used spray control parameters (namely, coating supply rate, shaping air pressure, gun-to-target distance, and coating viscosity). The immediate consequence of such

poor data availability is that process guidelines derived from available information will most likely fail to optimize inter-tablet coating uniformities. To address that lack, this study presents comprehensive spray data consisting of spatially resolved spray drop size, velocity, and volume flux and their variations with common spray parameters.

Materials and Methods

Sprays produced by two atomizers (Schlick 930 and 970) were characterized. Both were equipped with a flat-shaped air cap and an anti-bearding coating cap (ABC). Unlike conventional units, ABC-type caps protrude several mm past the atomizing air outlet (see Fig. 1). This feature is intended to prevent clogging due to coating buildup at the atomizing air outlet. The Schlick guns also feature separate shaping air and atomizing air inlets. Spraying conditions are summarized in Table 1. Unless otherwise noted, water is the sprayed coating.

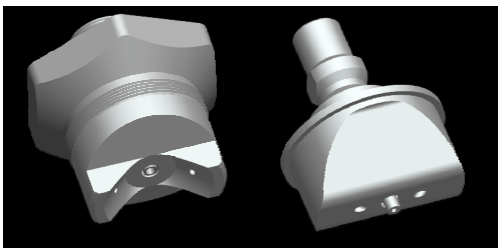

Figure 1. Illustrations of air/coating cap of (left) a traditional fan sprays-producing gun and (right) a Schlick gun

Mean drop size, velocity, and flux measurements for all sprays were made using a Dantec Dynamics dual-PDA. The operating principles, validation routines, and data processing algorithms are described in [13, 14]. The dual-PDA was used in the present study because it is less susceptible to Gaussian beam and slit effect sizing errors [13, 15, 16]. Furthermore, the dual-PDA system is significantly more accurate than standard three-detector systems, and is also slightly more accurate than the Qiu-Sommerfeld [17, 18] PDA system when used to measure mass flux [19].

Configuring a dual-PDA for measurement requires specifying values for the Processor, Group, PDA and LDA, and Optical PDA. One example of specification choice is to maximize the data rate. Another is to compromise between maximum data rate and maximum validation rate. A third possibility is to demonstrate mass closure for the spray of interest. We chose the latter because tracking spray mass is of significant importance in tablet coating.

Table 1. Spraying conditions used in experiments.

Condition	Gun	P_{AA} (kPa)	P_{SA} (kPa)	$\dot{m}_{liq}$ (g/min)	Gun-to-Target Distance (cm)	Data shown in
1	Schlick 930	205	140	80	14	Fig. 2a
2	Schlick 930	275	140	80	14	Fig. 2b
3	Schlick 930	275	210	80	14	Fig. 2c
4	Schlick 930	275	140	110	14	Fig. 2d
5	Schlick 930	275	140	110	16.5	Fig. 2e
6	Schlick 970	140	140	80	14	Fig. 3a
7	Schlick 970	205	140	80	14	Fig. 3b
8	Schlick 970	205	205	80	14	Fig. 3c
9	Schlick 970	140	140	110	14	Fig. 3d
10	Schlick 970	140	140	110	16.5	Fig. 3e

Mass (volume) closure was achieved in the following manner. The coating volume flow rate entering an atomizer was measured using a MicroMotion FO25S Coriolis flow meter. The dual-PDA was then used to acquire spatially resolved drop size, velocity and volume flux data on a 5 mm x 5 mm grid. Spray volume flux was then determined by multiplying all local volume flux values by their corresponding grid areas. Subsequent spatially resolved measurement sets were acquired while adjusting LDA/PDA and optical PDA selections until the PDA-calculated and MicroMotion-measured volume flow rates were within 10% of each other. Such a validation criterion was satisfied by closely following the dual-PDA operating guidelines presented in [20]. In particular, measurements were performed by using a relatively low PMT voltage (700-800 V) and gain (0 db), and by truncating the width of the burst signals to a fixed length that corresponds to approximately half the width of the burst signal at the most dense point in the spray. PDA data obtained in this manner have been shown to agree to within ~20% of data from an En'Urga Inc. OP-600, an extinction-based optical patternator [20].

Results and Discussion

Drop size, velocity, and volume flux data for all conditions are shown in Figs. 2 and 3 for, respectively, the 930 and 970 sprays. The separate effects of varying atomizing air pressure, shaping air pressure, coating supply rate, gun-to-target distance, and coating viscosity are discussed below.

The effects of increasing atomizing air pressure on drop size, axial velocity, and volume flux are seen by comparing Fig. 2a with 2b for the 930 spray and by comparing Fig. 3a with 3b for the 970 spray. Drop size data show the expected decrease as atomizing air pressure increases. Note that drop diameter is smallest at locations close to the spray center for both sprays, due to the ballistic nature of large drops.

The middle column of Figs. 2a,b and 3a,b shows corresponding velocity maps. The elliptical pattern is expected, and is due to the shaping air flow; the expected increase in velocity occurs when atomizing air pressure rises. Drop velocity data also suggest that increasing atomizing air supply pressure decreases spray cone angle. This may be due to the reduction in drop size, along with the realization that smaller drops are more susceptible to entrained air-induced drag that drives them toward the spray center.

The reduction in spray extent is supported by the volume flux distributions (the rightmost columns of Figs. 2a,b and 3a,b). Note that spray volume flux is highest near the location where the drop velocity is maximum. This is expected. Accordingly, local volume flux increases as atomizing air pressure increases.

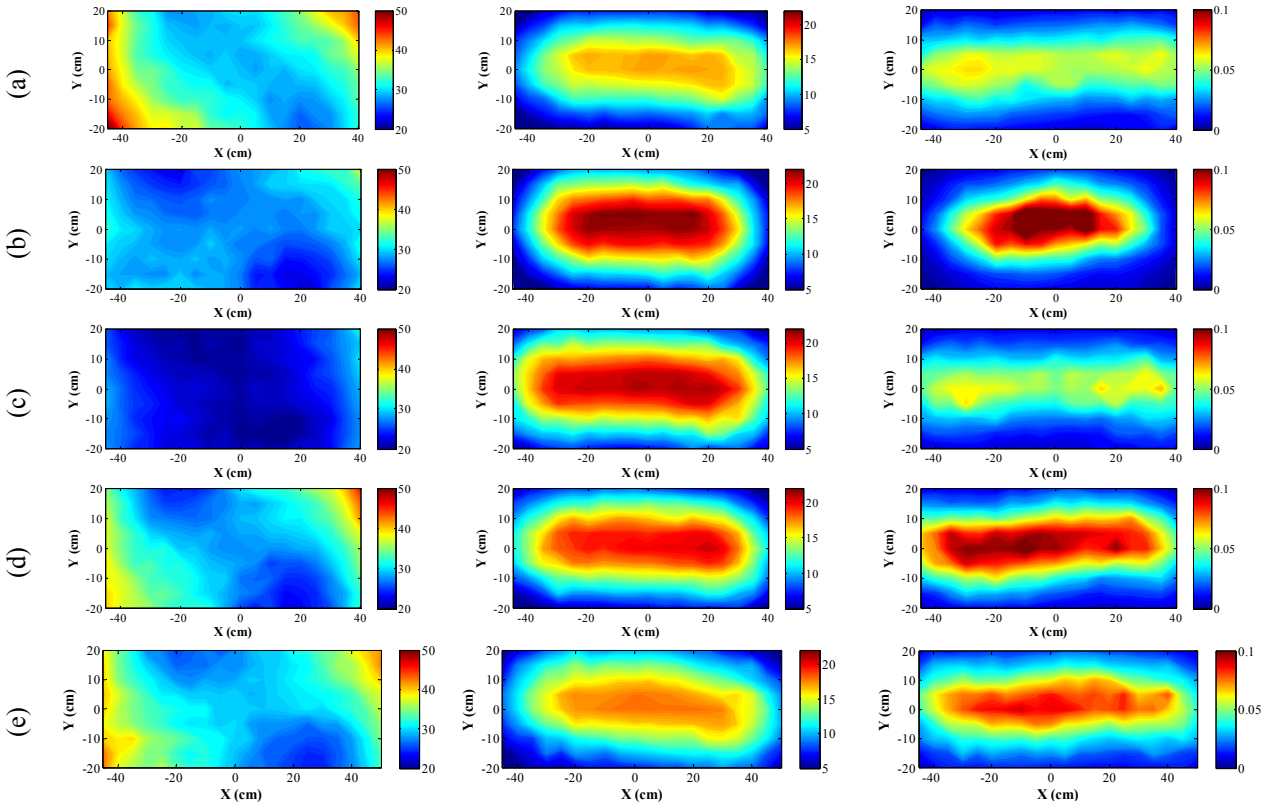

Figure 2. (left) Diameter, (middle) velocity, and (right) volume flux data for the Schlick 930 sprays

Comparison of volume flux profiles in Figs. 2a and 2b to those in Figs. 3a and 3b shows that the two sprays 'react' differently to an increase in atomizing air pressure. Volume flux data in Fig. 2a show that the 930 spray is somewhat uniform with no distinct localized peaks when the gun is operated at the lower atomizing air pressure (205 kPa). This suggests that a largely uniform spray can be produced when there is a balance between atomizing air pressure, shaping air pressure, and coating supply rate. As atomizing air pressure rises, however, the spray becomes more circular and develops a local peak at the spray center (third column of Fig. 2b). This is expected because of the increase in drop velocity accompanying the increase in atomizing air pressure, as shown in the middle column of Fig. 2b, and because data rates at the spray center increase as atomizing air pressure increases, suggesting that drop concentrations at the spray center increase as well. The combination increases volume flux at the center.

In contrast, the 970 spray changes from a dumbbell to a teardrop pattern as atomizing air pressure rises. The dumbbell pattern is likely the result of spray 'pinching' that occurs due to the shaping air. This effect was observed

whenever the radial momentum along the spray's semi-minor axis (due to shaping air) exceeds the axial momentum (due to atomizing air) by a certain amount. Interestingly, even when the dumbbell pattern is avoided, the 970 spray drop velocity and volume flux profiles are never symmetric. This might be due to manufacturing defects.

The influences of shaping air pressure on drop size, axial velocity, and volume flux can be seen by comparing Figs. 2b to 2c for the 930 sprays, and by comparing Figs. 3b to 3c for 970 sprays. Drop size data show that drop diameter decreases as shaping air pressure increases; more significantly so for the 930 spray than for the 970 one. The shaping air velocities for both guns, as measured using PIV 2 mm downstream from the outlets, are approximately 260 m/s. Assuming a drop size of 18 μm (the smallest D_{32} observed in Figs. 2 and 3), *We* can be calculated to be ~20, which is well above the critical We limit (~12). As such, the decrease in size accompanying an increase in shaping air pressure is likely arising from secondary droplet atomization.

An increase in shaping air pressure leads to a slight decrease in axial drop velocity for the 930 spray. This is unexpected and is likely related to the decrease in size with increasing shaping air pressure (see above). Smaller droplets lose their momentum rapidly, leading to the observed decrease in velocity. Note that the decrease in drop axial velocity is not observed in the 970 spray data. This is expected, as the decrease in size accompanying an increase in shaping air pressure for the 970 spray is not as significant as for the 930 spray.

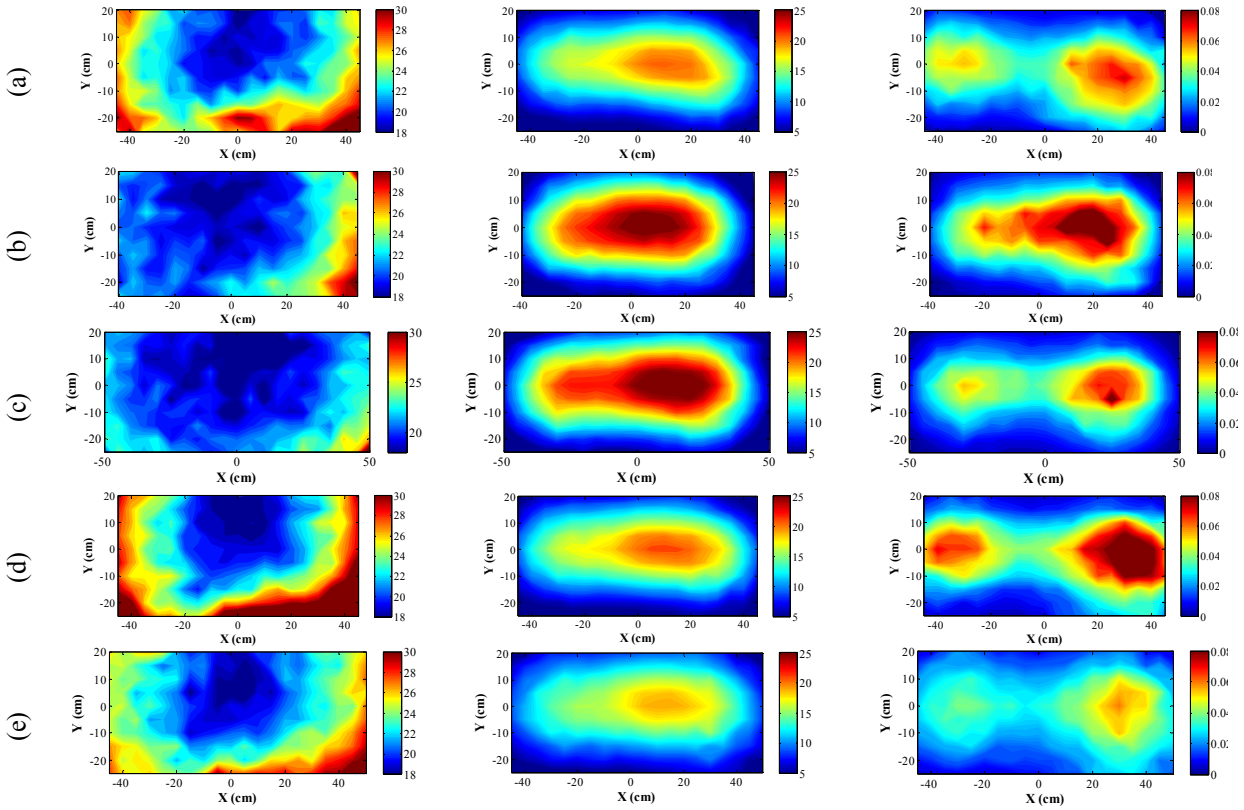

Figure 3. (left) Diameter, (middle) velocity, and (right) volume flux data for the Schlick 970 sprays

Comparison of volume flux data in Figs. 3b and 3c shows that both sprays become more elliptical as shaping air pressure rises. This result is also in agreement with the drop velocity data (middle column in Figs. 2b,c and 3b,c). For the 970 spray, the increase in spray extent is also accompanied by the development of dumbbell-shaped volume flux profile. Furthermore, as a result of a more dispersed spray, the local volume flux magnitude decreases with an increase in shaping air pressure. The volume flux profiles for 930 sprays, on the other hand, display a single peak at the spray center at lower shaping air pressure (140 kPa). Interestingly, the overall volume flux profile becomes largely uniform (no discernable localized peak) as shaping air pressure rises to 210 kPa.

The effects of increasing coating supply rate on spray characteristics can be seen by comparing Figs. 2b and 2d for the 930 spray and Figs. 3a and 3d for the 970 spray. Drop size data show a modest increase in drop size, particularly at the spray periphery, as coating supply rate increases. This is expected and is due to the increase in coating supply rate, which results in larger ligaments and ultimately leads to larger drops. Increasing the coating supply rate for the 970 sprays also increases drop size, but the effect is much less pronounced than for the 930

sprays. This may be explained by considering the PIV-measured atomizing air velocities for the two different guns. For the 930 gun operated at 275 kPa, the atomizing air velocity is at most 140 m/s. For the 970 gun operated at 140 kPa, the atomizing air velocity is as high as 280 m/s. These data suggest that the 970 gun provides more efficient atomization than the 930 gun at the level of atomizing air pressure used.

Velocity distributions (middle column of Figs. 2b,d and 3a,d) and volume flux (rightmost column of Figs. 2b,d and 3a,d) show that both the 930 and 970 sprays become more elliptical with increasing coating supply rate. This is expected since the larger drops produced at higher coating mass flowrate are less prone to entrained air induced aerodynamic drag that would drive them toward the spray center. In addition, volume flux data also show an increase with increasing coating mass flow rate. This too, is expected since larger drops are being produced.

Volume flux and velocity measurement results again show that the two sprays respond differently to variations in coating supply rate. For the 970 spray, increasing the coating supply rate simply makes the spray wider (more elliptical). The overall spray pattern, however, is unchanged—it is still dumbbell-shaped. In contrast, for the 930 spray, increasing the coating supply rate shifts the peak location, apart from making the spray more elliptical.

Finally, drop velocities for the two sprays decrease as coating supply rate is increased. This is expected, as the increase in coating mass is not balanced by an increase in atomizing air so correspondingly less momentum is available to move the droplets downstream. Note that the decrease in drop velocity due to increasing coating supply rate is not as significant for the 970 sprays as it is for the 930 sprays. This is because the 970 gun provides more efficient atomization than the 930 gun at the level of atomizing air pressure tested, as discussed above.

The effects of increasing gun-to-target distance on drop size, axial velocity, and volume flux can be seen by comparing Figs. 2d and 2e for the 930 spray and Figs. 3d and 3e for the 970 spray. Drop size data show that an increase in gun-to-target distance has no significant effect on drop size. This suggests there was little evaporation. This may not represent an actual tablet coating process as drying air is often heated to ~60^{o}C.

Drop velocity data (middle columns of Figs. 2d,e – 3d,e) show the expected decrease with distance from the nozzle tip. Velocity and spray volume flux (rightmost columns of Figs. 2d,e – 3d,e) data also exhibit the expected spatial expansion as gun-to-target increases. An increase in gun-to-target distance also decreases spray volume flux. This is expected considering the decrease in drop velocity. Finally, it can be seen that, apart from increasing the spray extent, variations in gun-to-target distance have no significant effect on size, velocity, or flux, profiles in the two sprays (e.g. the location of maxima and minima in volume flux and velocity maps is unchanged).

The influence of coating formulation on spray drop size, axial velocity, and volume flux is shown in Fig. 4, where data obtained using 1.5, 2.5, and 3.5% w/w HPMC-E5 are shown for spray condition 1. The drop size increase as coating viscosity increases is expected since an increase in viscosity leads to larger drops for primary atomization dominated processes, and opposes aerodynamic induced breakup for secondary atomization processes.

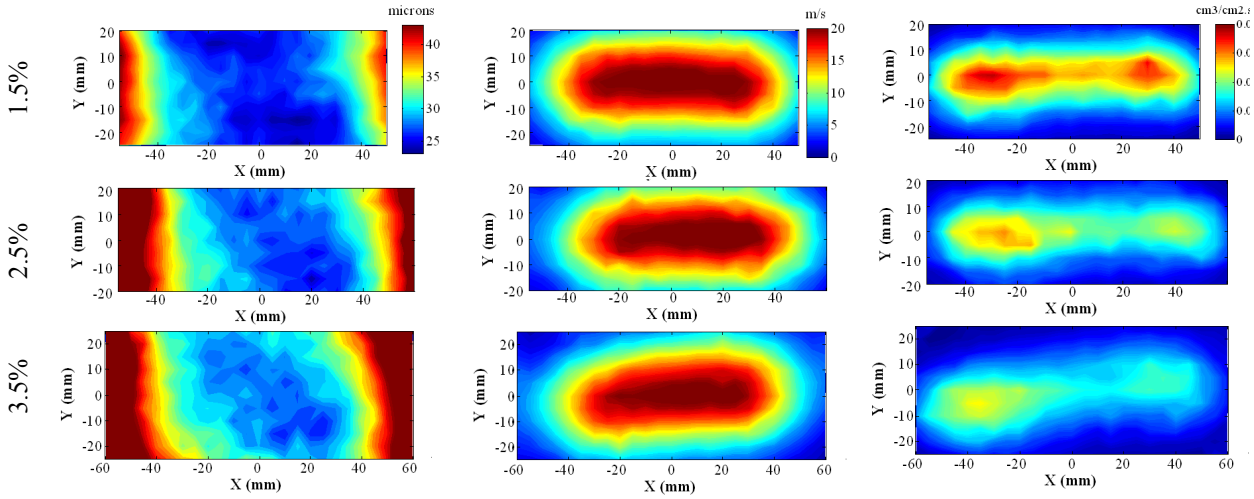

Figure 4. (left) drop diameter, (middle) velocity, and (right) volume flux data of HPMC sprays (condition 1)

Data in Fig. 4 also indicate that water sprays have the highest volume flux and that volume flux decreases as HPMC-E5 concentration increases. This can be explained by first realizing that drop sizes increase with formulation concentration. Since the coating supply rate is the same for all three sprays, and the velocities are not significantly different, spray drop concentration must decrease as drop sizes increase. A decrease in spray concentration means that the average number of drops per unit area decreases as well. This lowers spray volume flux.

Finally, it can be observed that more elliptical sprays result with an increase in coating viscosity. Also note that the dumbbell pattern develops as the spray widens, similar to the behavior of 970 sprays. The development of dumbbell patterns in this case is likely the result of the reduction in spray drop number density at the spray center.

Conclusions

Key conclusions are: (i) Drop size shows the expected increase with a decrease in atomizing air pressure, an increase in coating supply rate, and an increase in formulation concentration. It is unaffected by variations in gun-to-target distance; (ii) Drop velocity exhibits the expected increase with increasing atomizing air pressure. Shaping air pressure and coating supply rate have mixed effects—increasing the shaping air pressure slightly increases drop velocity for the Schlick 970 spray, but slightly decreases drop velocity for the Schlick 930 spray. An increase in coating supply rate, on the other hand, decreased drop velocities for the 930 sprays, but has no significant effect on 970 drop velocities; (iii) Local volume flux magnitude increase with an increase in coating supply rate, an increase in atomizing air pressure, a decrease in shaping air pressure, and a decrease in formulation concentration. All are expected. Depending on operating conditions, volume flux distributions show that typical pharmaceutical sprays have four possible patterns: elliptical with maxima located at two opposing ends of the spray (dumbbell-shaped), elliptical with maxima located several centimeters offset from the spray centerpoint (teardrop-shaped), elliptical with maxima located at the spray center (Gaussian), and elliptical with no distinct maxima.

Experimental data show that sprays produced by air-assist atomizers have non-uniform drop size, velocity, and flux distributions. These non-uniformities, however, can be reduced by adjusting the spray control parameters. For instance, for the Schlick 930 sprays, a largely uniform drop size distribution can be obtained by employing high level of atomizing air pressures. To minimize inter-tablet film thickness variabilities, dumbbell-, teardrop-, and Gaussian-shaped spray patterns must be avoided. For the Schlick 930 gun used in this study, this can be achieved by adjusting the shaping air pressure to within 0.7 – 0.8 of the atomizing air pressure. Care must be taken, however, when changing the liquid viscosity. As shown in Fig. 4 data, spray parameters that provide largely uniform spray pattern for water sprays result in dumbbell-shaped patterns when used for higher-viscosity liquids. This was hypothesized to result from a decrease in spray drop number density at the spray center. It is therefore recommended for manufacturing operators to always re-characterize the sprays whenever liquid viscosity changes.

References

1. Mowery, M. D., Sing, R., Kirsch, J., Razaghi, A., Bechard, S., and Reed, R. A., 2002, *Journal of Pharmaceutical and Biomedical Analysis*, 28(5), pp. 935-943.
2. Fisher, D. G., and Rowe, R. C., 1976, *Journal of Pharmacy and Pharmacology*, 28(12), pp. 886-889.
3. Rowe, R. C., 1981, *Journal of Pharmacy and Pharmacology*, 33, pp. 610-612.
4. Twitchell, A. M., 1990, "Studies on the Role of Atomisation in Aqueous Tablet Film Coating."
5. Rowe, R. C., and Forse, S. F., 1982, *Acta Pharmaceutica Technologica*, 28(3), pp. 207-210.
6. Tobiska, S., and Kleinebudde, P., 2003, *Pharmaceutical Development and Technology*, 8(1), pp. 39-46.
7. Rege, B. D., Gawel, J., and Kou, J. H., 2002, *International Journal of Pharmaceutics*, 237(1-2), pp. 87-94.
8. Porter, S. C., Verseput, R. P., and Cunningham, C. R., October 1997, *Pharmaceutical Technology*, pp. 1-7.
9. Aulton, M. E., 1995, "Surface Effects in Film Coating," Pharmaceutical Coating Technology, G. C. Cole, J. E. Hogan, and M. E. Aulton, eds.
10. Aulton, M. E., 1995, "Mechanical Properties of Film Coats," Pharmaceutical Coating Technology.
11. Rowe, R. C., and Forse, S. F., 1981, *Journal Of Pharmacy And Pharmacology*, 33, pp. 174-175.
12. Scattergood, L. K., Cunningham, C. R., Vesey, C. F., and Fegely, K. A., 2000, *3rd World Meeting APV/APVGI*Berlin.
13. Tropea, C., Xu, T. H., Onofri, F., Grehan, G., Haugen, P., and Stieglmeier, M., 1996, *Particle & Particle Systems Characterization*, 13(2), pp. 165-170.
14. Albrecht, H.-E., 2003, *Laser Doppler and Phase Doppler Measurement Techniques*, Springer, Berlin ; New York.
15. Durst, F., and Tropea, C., 1994, *Modern Techniques and Measurements in Fluid Flows*, pp. 38-43.
16. Xu, T. H., and Tropea, C., 1994, *Measurement Science & Technology*, 5(8), pp. 969-975.
17. Sommerfeld, M., and Qiu, H. H., 1995, *Experiments In Fluids*, 18(3), pp. 187-198.
18. Qiu, H. H., Sommerfeld, M., and Durst, F., 1994, *Measurement Science & Technology*, 5(7), pp. 769-778.
19. Dullenkopf, K., Willmann, M., Wittig, S., Schone, F., Stieglmeier, M., Tropea, C., and Mundo, C., 1998, *Particle & Particle Systems Characterization*, 15(2), pp. 81-89.
20. Muliadi, A. R., Sojka, P. E., Sivathanu, Y., and Lim, J., 2007, *2007 ASME International Mechanical Engineering Congress and Exposition*, ASME, Seattle, WA.